

MARIA S. MERIAN-Berichte

**BATHYMETRIC MAPPING OF THE SEAFLOOR – A GERMAN
CONTRIBUTION TO COMPLETING THE MAP BY 2030**

Cruise No. MSM88/1 + MSM88/2

November 28, 2019 – January 14, 2020

Mindelo (Cabo Verde) – Mindelo (Cabo Verde) – Bridgetown (Barbados)

GERMANMAPPING



Colin Devey, Anne-Cathrin Wölfl, Nico Augustin, Mary Besaw, Daniel Damaske, Dario Évora, Alexandra Gray, Christian Hübscher, Morgane Le Saout, Thorsten Lux, Martin Schade, Linda Sobolewski, Heinrich Villinger

Colin Devey (leg 1), Anne-Cathrin Wölfl (leg 2)
GEOMAR Helmholtz Centre for Ocean Research Kiel

2020

Table of Contents

1	Cruise Summary.....	3
1.1	Summary in English.....	3
1.2	Zusammenfassung.....	3
2	Participants.....	4
2.1	Principal Investigators	4
2.2	Scientific Party	4
2.3	Participating Institutions	4
3	Research Program	6
3.1	Description of the Work Area.....	6
3.2	Aims of the Cruise	6
3.3	Agenda of the Cruise	8
4	Narrative of the Cruise	10
5	Preliminary Results	11
5.1	Hydroacoustics.....	11
5.1.1	System Overview and Data Processing	11
5.2	Magnetic Measurements	12
5.2.1	System Overview	12
6	Station List MSM88.....	15
6.1	Overall Station List	15
7	Data and Sample Storage and Availability	18
8	Acknowledgements.....	19
9	References.....	20
10	Abbreviations	21
11	Appendix - Selected Pictures of Samples	22

1 Cruise Summary

1.1 Summary in English

Despite over 100 years of acoustic seabed mapping, only around 15% of the seafloor has ever been directly mapped and little of the mapping performed has been systematic or over larger areas. The result is that our knowledge of seafloor structure is rudimentary and our understanding of the processes which form them has, in principle, advanced little since the advent of plate tectonics. Societally, the seafloor plays a vital role in humanity's "life support system", for example providing habitat for marine organisms, stimulating mixing of ocean water as part of the overturning circulation system and increasingly being the site of industrial installations. It is scientifically and societally imperative that we bring the level of knowledge of the surface of our planet up to that of bodies like Moon and Mars that are mapped with a resolution better than 100 m per pixel. It is also essential that the data are made freely available to all to support research and conservation. The aim of this cruise was to map previously uncharted part of the tropical Atlantic using the ship's multibeam system and to provide the data to global open databases as well as to acquire magnetic gradient data along the same tracks. Magnetic anomalies from so-called Oceanic Core Complexes challenged the conventional view that marine magnetic anomalies arose in the upper, extrusive layer of the oceanic crust, because the crust has been stripped away at these complexes. We therefore collected magnetic data simultaneously to the multibeam data in order to constrain the interpretation of the observed seabed morphology.

1.2 Zusammenfassung

Obwohl schon seit über 100 Jahren die Meeresböden der Weltmeere mit hydroakustischen Methoden vermessen werden, sind bisher nur ungefähr 15% des Meeresbodens direkt kartiert worden. Die Konsequenz, die sich daraus ergibt, ist ein lückenhaftes Wissen über die Topographie unserer Meeresböden. Auch unser Verständnis über die dort vorkommenden Prozesse haben sich seit Entdeckung der Plattentektonik nur marginal weiterentwickelt. Gesellschaftlich spielt der Meeresboden eine entscheidende Rolle im „Lebenserhaltungssystem“ der Menschheit, z.B. als Lebensraum für marine Lebewesen, durch seinen Einfluss auf Meeresströmungen, und auch vermehrt als Standort für Industrieanlagen. Es ist für den wissenschaftlichen und gesellschaftlichen Fortschritt unerlässlich, dass wir das Wissen über die Oberfläche unseres Planeten auf den Wissensstand von Mond und Mars bringen, die mit einer Auflösung von weniger als 100 m pro Pixel kartiert sind. Es ist ebenfalls erforderlich, dass Daten frei zugänglich gemacht werden um Forschung und Meeresschutz weiter voran zu bringen. Ziel dieser Fahrt war es, einen bisher größtenteils unerforschten Teil des tropischen Atlantiks mithilfe eines schiffsbasierten Fächerecholots zu kartieren und die Daten in internationalen Datenzentren uneingeschränkt zur Verfügung zu stellen. Ebenfalls wurden entlang der Profile magnetische Messungen durchgeführt. Magnetische Anomalien von sog. Ozeanischen Kernkomplexen ließen Zweifel an der bisher gültigen Annahme entstehen, dass die magnetischen Anomalien ihren Ursprung in den extrudierten, oberen Lagen der ozeanischen Kruste haben, da diese dort nicht mehr existent ist. Um den Interpretationsspielraum der bathymetrischen Strukturen einzuschränken, wurden magnetische Daten zusätzlich entlang der Fächerecholotprofile aufgenommen.

2 Participants

2.1 Principal Investigators

Name	Institution
Leg 1	GEOMAR
Devey, Colin, Prof. Dr.	
Leg 2	
Wölfel, Anne-Cathrin, Dr.	GEOMAR
Hübscher, Christian, Prof. Dr. (Onshore)	IfG-HH

2.2 Scientific Party

Name	Discipline	Institution
Leg 1		
Devey, Colin, Prof. Dr.	Bathymetry / Chief Scientist	GEOMAR
Augustin, Nico, Dr.	Bathymetry	GEOMAR
Évora, Dario	Bathymetry	IMar
Gray, Alexandra	Bathymetry	uOttawa
Sobolewski, Linda	Bathymetry	RUB
Leg 2		
Wölfel, Anne-Cathrin, Dr.	Bathymetry / Chief Scientist	GEOMAR
Besaw, Mary	Bathymetry	uOttawa
Damaske, Daniel	Bathymetry	MARUM
Le Saout, Morgane, Dr.	Bathymetry	GEOMAR
Lux, Thorsten	Bathymetry	GEOMAR
Schade, Martin	Bathymetry	GEOMAR
Villinger, Heinrich, Prof. Dr.	Geophysics	GEOMAR

2.3 Participating Institutions

GEOMAR Helmholtz Zentrum für Ozeanforschung Kiel
Wischhofstraße 1-3
24105 Kiel
www.geomar.de

IfG-HH – Institute for Geophysics, University of Hamburg
Bundesstrasse 55
20146 Hamburg
www.geo.uni-hamburg.de/en/geophysik.html

IMar - Instituto do Mar
Cova de Inglesa
C.P. 132
Mindelo
Cabo Verde
www.facebook.com/INDP.CV/

uOttawa - Université d'Ottawa | University of Ottawa
75 Laurier Ave. East
Ottawa ON K1N 6N5
Canada
www.uottawa.ca

RUB - Ruhr-Universität Bochum
Universitätsstraße 150
44801 Bochum
www.ruhr-uni-bochum.de

MARUM - Center for Marine Environmental Sciences University Bremen
Leobener Strasse 2
28359 Bremen
www.marum.de



MSM 88 Leg 1



Colin Devey
Chief Scientist



Nico Augustin
Scientist



Linda Sobolewski
Scientist



Dario Évora
Scientist



Alexandra Gray
Scientist

MSM88-2



Anne-Cathrin Wölfli
Chief Scientist



Morgane Le Saout



Thorsten Lux



Mary Besaw



Heiner Villinger



Martin Schade



Daniel Damaske

3 Research Program

3.1 Description of the Work Area

The work area is situated between 14° and 17° North and stretches from the exclusive economic zone (EEZ) of Cabo Verde in the east to the Guadeloupean and Martinican EEZ in the west and covers only international waters. Most of the work area has not been surveyed with hydroacoustics, except for some transit lines and the region at and around the Mid-Atlantic Ridge (MAR). The MAR is one of the most prominent features in the working area that has shaped and still shapes the seafloor in the Atlantic Ocean. Beside the ridge axis occur smaller ridges and fracture zones, seamounts as well as flat plains in the work area.

3.2 Aims of the Cruise

The present state of seafloor mapping, based on the data holdings of the IHO Data Centre for Digital Bathymetry (DCDB) hosted at NOAA's NCEI, is shown in Figure 3.1. With the exception of the US EEZ and some regions of the Mid-Atlantic Ridge (MAR), most of the Atlantic Basin has only ever been imaged on single, widespread lines. Particularly the eastern Atlantic (east of the MAR) is virtually unsurveyed. The greyscale "background" map represents an estimation of the bathymetry from satellite altimetry (Sandwell and Smith, 1997). This estimation has a horizontal resolution of >1km and comparison of altimetry and multibeam data from the same area shows a significant coherence of the data (coherence >0.5, where coherence is the square of the linear correlation coefficient as a function of wavelength, a coherence of 0.5 implies a signal:noise ratio of 1:1) only at wavelengths >2km (Marks et al., 2013). In well-surveyed areas, differences between estimated and measured water depths are known to exceed 1900m (Picard et al., 2018), with the errors increasing in regions of rough topography, characteristic of slowly spreading crust such as in the Atlantic. As a result, in terms of seafloor structure the altimetry maps show only the most fundamental tectonic structures and their resolution is particularly poor in basins like the Atlantic. An illustration of this is shown in Figure 3.2.

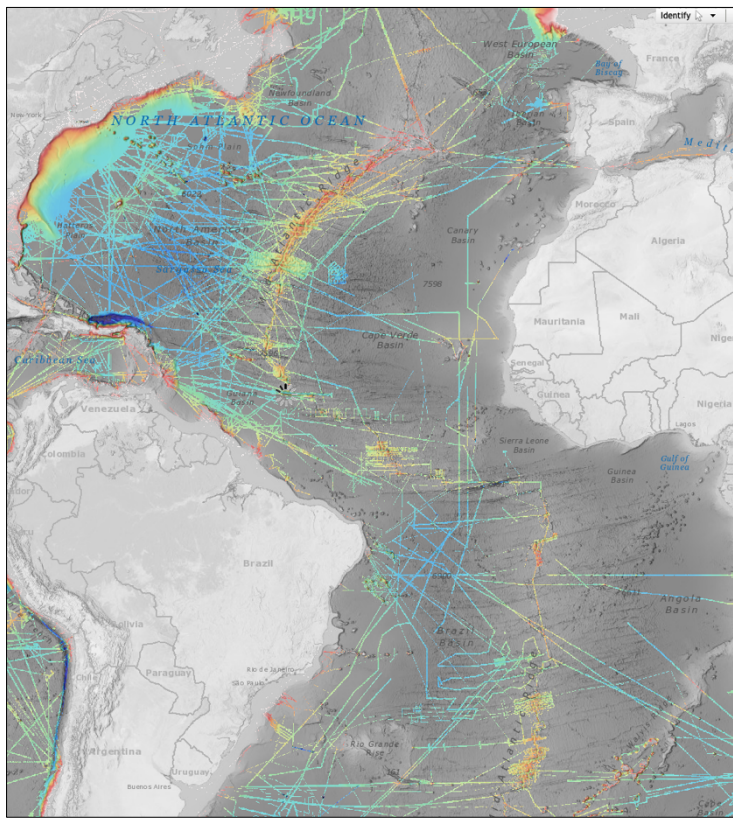


Figure 3.1: The current state of seafloor mapping in the Atlantic based on IHO data holdings. Although some regions (especially in national EEZ) may also have been mapped without the data being made publically available (Ireland is a notable exception in this regard) this map represents what is openly known about the shape of the Atlantic seafloor.

Attempts to change this situation have begun internationally (e.g. Mayer et al., 2018; Wölfel et al., 2019) and also regionally, with the EU, US and Canada focusing on the North Atlantic and attempting to prioritize areas to map in the vast uncharted regions of the oceans (ca. 300.000.000 km² remain to be mapped). Wölfel et al. (2017) used a GIS-based analysis, taking into account, e.g. marine protected areas, seafloor installations and even trans-Atlantic flight corridors to propose such a prioritization. They noted that one of the problems with such an approach is that areas without data often do not show up in categories like "Marine protected area" as such protected areas are not established when basic data like bathymetry are not available - a "Catch 22" situation. Wölfel et al. stated "we [...] stress that all relatively unmapped regions [...] warrant further study as at present so little information is available that we cannot accurately assess their environmental or resource relevance". Our initial work on this problem has resulted in the establishment, in collaboration with the German Research Fleet Coordination Centre (Leitstelle Deutsche Forschungsschiffe) of an "underway bathymetry" procedure for all German High Seas research vessels, resulting up to present in the publication of 65 data sets or their products in the World Data Centre PANGAEA (databank query on 10.03.2020, keywords "AtlantOS" AND "Wölfel, Anne-Cathrin"). The bathymetry dataset obtained on MSM88 will also be freely available at PANGAEA as well as at the IHO DCDB, from where it will be integrated into the GEBCO chart series. This will be by far the largest "underway bathymetry" data set ever made publically available.

The simultaneously carried out magnetic mapping mainly aimed on studying oceanic core complexes (OCC), also called megamullions. Magnetic anomalies from The Kane Megamullion near the Mid-Atlantic Ridge showed no significant change in character from the adjacent, normal crust (Tivey et al., 2004). This was not expected, because the primary location of crustal magnetization has been considered to be the volcanic layer (e.g., Talwani et al., 1971; Harrison, 1987). However, the detachment model and limited previous seafloor observations predict that a megamullion is exhumed sub-volcanic crust and upper mantle. Tivey et al. (2004) explained the presence of magnetic anomalies over Kane megamullion by a magnetized gabbro section. A recent study of crustal magnetization on the west flank of the MAR (Tivey and Tucholke, 1998) suggests that most magnetization in the volcanic layer is attenuated immediately off-axis and that lower crust and upper-mantle serpentinites may be a major contributor to the ridge-flank magnetic anomaly signal at slow-spreading ridges. Reversely magnetized gabbros have been drilled at Atlantis Bank megamullion on the Southwest Indian Ridge, and a minor reversal boundary that may correlate with the geomagnetic time scale has been identified (Allerton and Tivey, 1998).

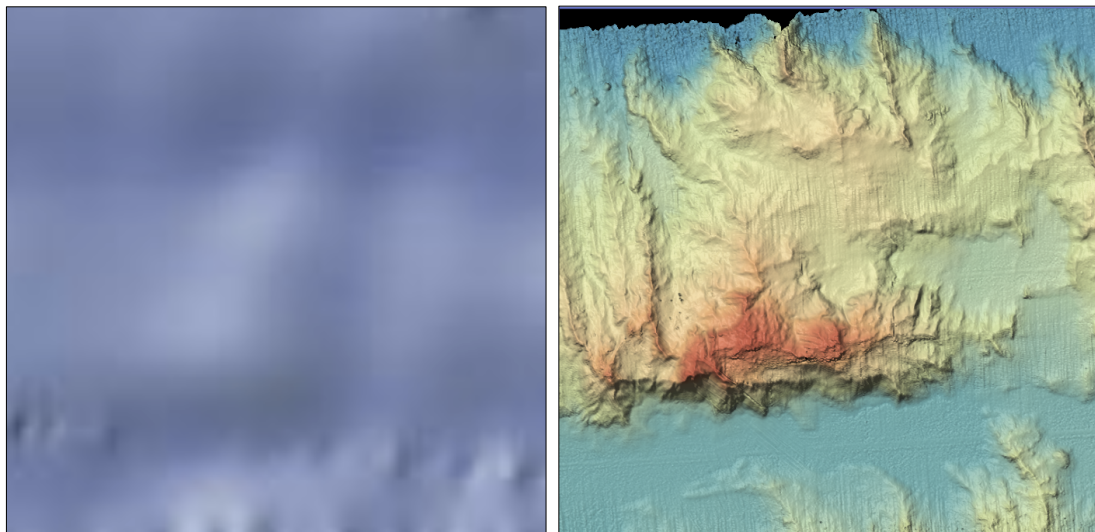


Figure 3.2: A 50x50km area of the Atlantic seafloor imaged by satellite altimetry (left) and by a ship-mounted multibeam system (right, from SO-237). Detailed geological and marine habitat interpretations are only possible with the multibeam image.

3.3 Agenda of the Cruise

The cruise consisted of 7 long profiles, where bathymetric, magnetic and sub-bottom data was obtained (Fig. 3.3). Altogether we measured four sound velocity profiles through the water column to calibrate the depth measurements. Two were measured at the eastern edges of profile 1 and profile 2, one was measured at the western edge of profile 1 and one was measured close to the Mid-Atlantic Ridge. The ship's ADCP and thermosaligraph also ran permanently during the mapping to test for interference from the multibeam echosounder on the former and for the German Marine Research Alliance (DAM) pilot project Underway Research Data.

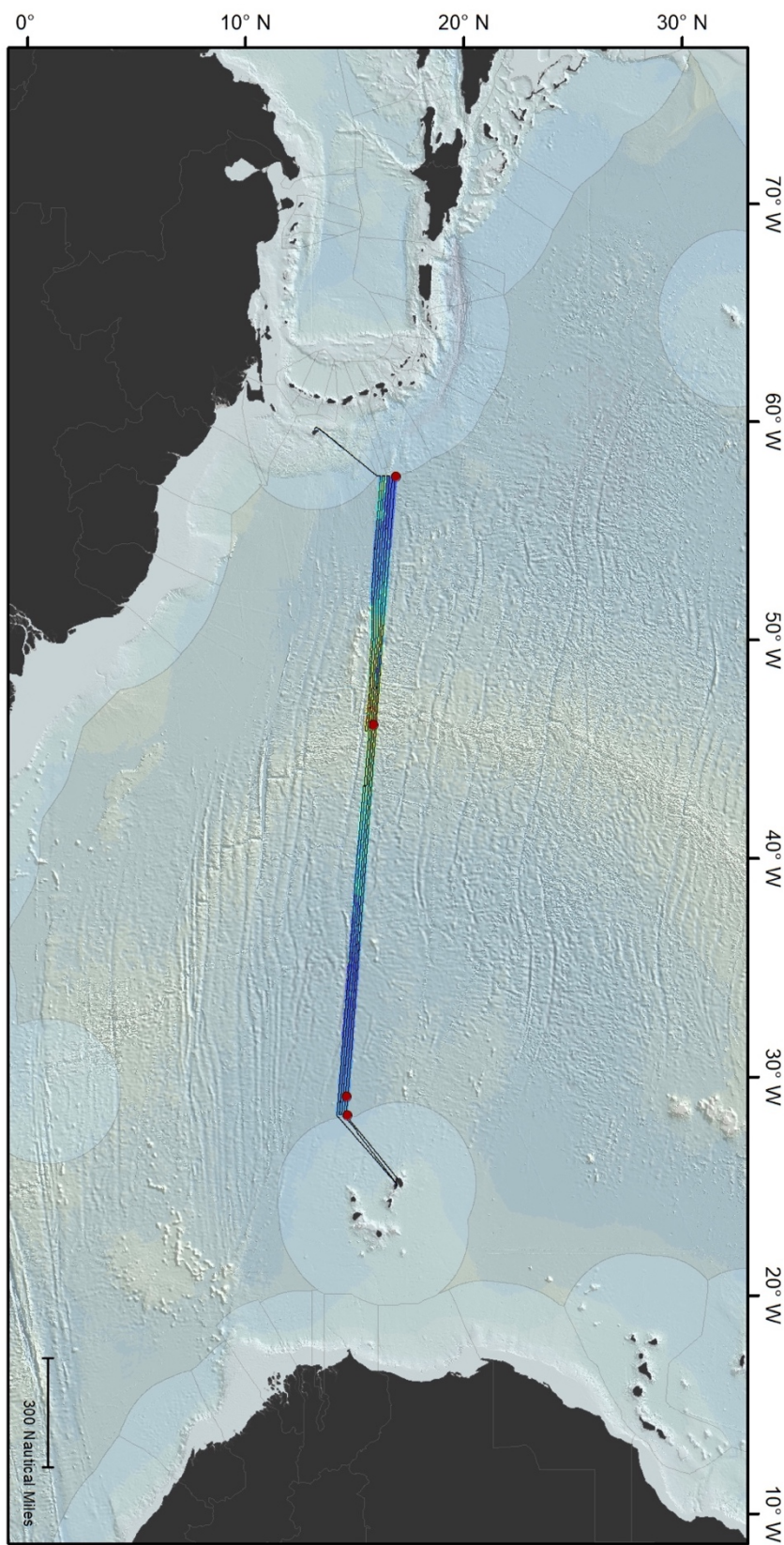


Figure 3.1: Cruise track during cruise MSM88 (black lines) and sound velocity measurements (red dots).

4 Narrative of the Cruise

Leg 1

(C. Devey)

RV MARIA S. MERIAN left the port of Mindelo punctually at 09:00 (UTC) on 28.11.19 and took a south-westerly course to reach the edge of the Cape Verdean Exclusive Economic Zone where the "German Mapping" work was to begin. We arrived in the working area at 04:00 on 29.11.19 and began our mapping work. At 09:00 on the same day we interrupted our profile to perform a sound-velocity profile (SVP). As the cruise is part of the DAM (Deutsche Allianz Meeresforschung) pilot project underway research data, we began running not only the EM122 multibeam echosounder, but also the acoustic doppler current profiler (ADCP) and the thermosalinograph. In addition, we were also collecting subsidiary data using a sub-bottom profiler and a magnetometer. The first of our 4 profiles was ca. 1140 nautical miles long and was completed on 03.12.19 at 01:00. Profile 2 began at 02:00 on the same day after a large-radius turn and continued until 13:00, when the magnetometer was recovered for a weekly check and the chance was used to perform a SVP to 3000m water depth. With the SVP completed we recommenced the bathymetry/magnetic profile 2 at 16:00 on 03.12.19. Profile 2 ended on 8.12.19 at 22:00, another large-radius turn took us on to profile 3, which we ended at 17:00 on 12.12.19. Once more we returned to an easterly course and began profile 4. This profile was completed on 16.12.19 at 11:00, at which point we were on the Cape Verde EEZ boundary, recovered the magnetometer and stopped pinging and recording multibeam data and began the transit back to Mindelo. We arrived alongside in Mindelo on 17.12.19 at 08:00.

Leg 2

(A.-C. Wölfel)

The second leg of the cruise started on 19.12.19 at 09:00 (UTC), when RV MARIA S. MERIAN left Mindelo harbour and arrived at the first working station in international waters early on 20.12.19. This station was located just outside the Cape Verdean Exclusive Economic Zone and north of the first profile from the previous leg. We measured a sound-velocity profile (SVP) and subsequently started at 10:35 to run the EM122 multibeam echosounder on our first 1700 nautical miles long profile, with a speed of 10 knots, heading towards the northwest. Similar to the previous leg, we were also collecting subsidiary data including magnetic field characteristics of the oceanic crust using a magnetometer, sub-bottom characteristics using a sub-bottom profiler as well as temperature and conductivity using a thermosalinograph and current velocities using an acoustic doppler current profiler (ADCP). On 27.12.19 at 04:20, at the end of profile 1, close to the Guadeloupean EEZ, another SVP was taken. After turning we started recording profile 2 at 07:30 with a length of approximately 600 nautical miles. At the end of this profile, we closed the gap to the MSM88/1 data on 30.12.19 at 04:35 and turned again westwards to finish profile 3. Profile 4 starting on 01.01.20 at 01:35 and profile 5 starting on 05.01.20 at 00:50, were approximately 800 nautical miles long and crossed the ridge axis again two more times. Profile 6 started on 08.01.20 at 11:50 and crossed the ridge axis again, before we had to turn and started our last profile 7 on 11.01.20 at 09:45, increasing the speed to 12.5 knots in order to arrive on time to the port of Bridgetown. We arrived to Bridgetown on 14.01.20 at 12:00.

5 Preliminary Results

(C. Devey, A.-C. Wölfel, N. Augustin, M. Le Saout, M. Schade, H. Villinger)

5.1 Hydroacoustics

5.1.1 System Overview and Data Processing

Multibeam Bathymetry and Backscatter

During cruise MSM88-1 the hull-mounted Kongsberg Maritime Simrad EM122 multibeam echo sounder of RV MARIA S. MERIAN was used throughout the entire cruise to record both bathymetric and backscatter data. The system operates at 12 kHz and covers water depths from 20 m below the transducers up to full ocean depth. Data acquisition was set to equidistant and multiping mode with the FM (chirp modulated) pulse enabled. Swath width was reduced to 100-120° total swath, except for the few occasions when crossing the shallower parts of the Mid-Atlantic Ridge (MAR) and a 150° swath was required. The Simrad EM122 system produces 432 beams, regardless of the swath width. Four sound velocity profiles were obtained using a sound velocity probe. However, water masses appeared to be stable throughout the working area and cruise duration. Data quality was good despite high waves (2-3 m swell from NE) most of the time producing some bad pings, and typical problems with the bottom detect algorithm on steep flanks facing away from the ship. The signal amplitude is also stored and preprocessed automatically by the Kongsberg acquisition software SIS. This preprocessing includes altitude processing and the application of time and angle varying gain functions. Water column data were not recorded during the cruise. A total of approximately 250,000 km² were mapped during the cruise. Data processing was carried out onboard using QPS Qimera 2.0.3 on MacOS. The standard procedure was to use a spline and outlier filter to initially clean the data and eliminate the worst outliers. The filter was complemented by manual editing in the 3D Editor to remove remaining outliers that were not detected automatically. The edited soundings were then gridded with Qimera for a 100m grid cell size. Backscatter data were processed using FMGeocoder, where radiometric corrections, angle-varying gain and anti-aliasing filters are applied, and a georeferenced mosaic is produced. Overall the processing of the bathymetric data was finished during the cruise.

Parasound

The PARASOUND system was used simultaneously to the EM122 multibeam throughout the cruise. The hull-mounted ATLAS PARASOUND P70 system is a deep-sea parametric sub-bottom profiler which utilizes the parametric effect based on a non-linear relation of pressure and density during sonar propagation. Two different waves with frequencies of ~18-20 kHz (primary high frequency, PHF) and a ~22-24 kHz wave was used to create a so-called secondary high (about 40-42 kHz, SHF) and a secondary low frequency (SLF) of about 4 kHz. Only the SLF is used for the sub-bottom profiling while the SHF can be used for water column imaging. The opening angle of the transducer array is 4° by 5°, which corresponds to a footprint size of about 7% of the water depth. The ATLAS PARASTORE program is used for storing and displaying echograms, while the program ATLAS Hydromap Control (AHC) is used to set proper hydroacoustic settings during acquisition. During the PARASOUND operations, data are recorded and stored as vendor-

specified *.asd files. Along with the raw ps3-files, auxiliary data files were recorded for a user-specified depth window. Water depth is hereby calculated from acoustic travel times using a constant sound speed of water of 1500 m/s. PARASOUND data were acquired along all multibeam profiles. Despite the large water depths and the steady waves from NE, the data are of good quality, best within deep sedimentary basins with low seafloor relief. Examples from the acquisition window (ParaStore) are shown in Figure 4.1. The sub-bottom imaging at steep slopes and hard bottom was challenging because there the sub-seafloor penetration of the acoustic signals was impossible. The obtained PARASOUND data were only stored and no further post-processing was performed. They are available for processing and interpretation after the cruise.

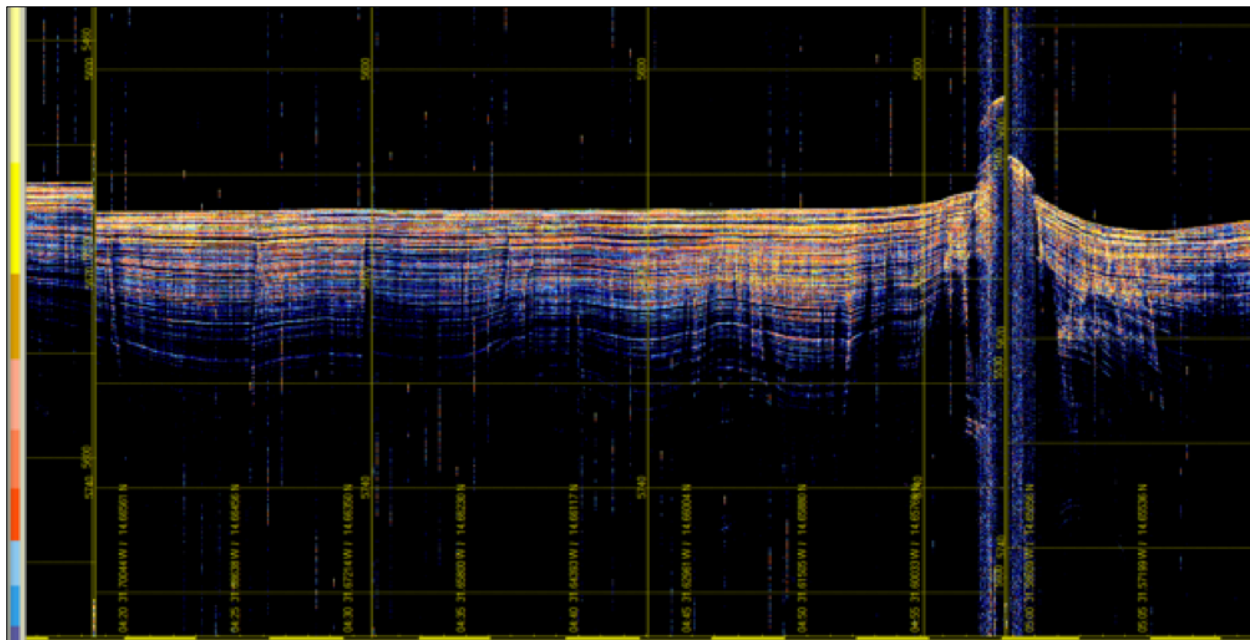


Figure 4.1: Sample of PARASOUND SLF echogram, in the eastern part of the working area (31.6°W) where the seafloor relief is low due to the older age of the crust and higher degrees of sedimentation. The depth of the lowermost signals is about 80 m below the seafloor.

5.2 Magnetic Measurements

5.2.1 System Overview and Data Processing

The magnetic data collected during MSM88-1 were acquired using a SeaSPY longitudinal gradiometer configuration. Two magnetometers were towed in a distance of approx. 300 m behind the vessel. The cable used to tow the magnetometers was deployed from a winch. The recording station was set up in the hydroacoustic lab and acquisition was performed using the BOB software. The acquisition software crashed relatively regularly (ca. once per day) and needed to be restarted which usually took a few minutes only. Navigational data were provided to BOB as NMEA telegrams via the ships internal network. Total offset from the first magnetometer tow-fish to the GPS antenna (layback) was set to 350 m. The magnetometer was in-between the cruise checked for damages with no issues. However, after finishing the last profile and recovering the magnetometers at the end of the research program of MSM88-1 we found the rear tow-fish damaged, presumably by a shark attack. The rubber coating was damaged, and one fin ripped off

(Figure 5.1). Further the magnetometer seemed to work fine. SeaSPY is a high sensitivity total field magnetometer packaged in a rugged marine housing. The measurement of the magnetic field is done inside the towed fish, while the tow cable supplied power to the towfish and a bi-directional digital communication link. The main sensor of the system is an Overhauser total field sensor. It operates on the proton spin resonance principle. A proton-rich liquid within the sensor is engineered in a way to allow a principle known as the Overhauser effect to occur within it. The sensor measures the magnetic flux density, which is measured in Tesla [T]. The distance between both magnetometers was 100 m. The towing depth was influenced by the speed of the vessel, which resulted in a towing depth of approx. 6 m. During our measurements the speed of the vessel was kept to ~ 10 kn. The sampling rate was initially set to 1 Hz but later reduced to 0.2 Hz (5 sec) due to the large water depths. The positions as well as the measured values were displayed in real-time on the acquisition software. The magnetic data have been only recorded during cruise and, apart from some test-plots for general control of the recorded data (Figure 5) no further processing was done during MSM88-1. The magnetic data will be evaluated and interpreted after the cruise.



Figure 5.1: Damaged rear tow-fish after a shark attack. The magnetometer is fully functional but the rubber coating was damaged and one fin missing.

The damage of the second tow-fish was so severe, that it was not used anymore during MSM88/2, hence no gradient measurements could be made. All measurements were made with 0.2 Hz (5 second period). Data from MSM88/1 profiles are severely affected by noise and had to be smoothed using a 5-minute moving average window. Still some noise is clearly visible which may be reduced by further processing. Data quality of the measurements during MSM88/2 was very good with a noise level below 1 nT. Therefore, no filtering or smoothing was required. The magnetic anomaly for all profiles was calculated by subtracting the IGRF (International Geomagnetic Reference Field) from our measured values. The IGRF is based on the coefficients for the period 2015 to 2020. The stacked profiles (Figure 5.2) show the excellent agreement between the data of the two legs except where profile MSM88/1-P3 meets profile MSM88/2-P4. The reason for this offset is unclear.

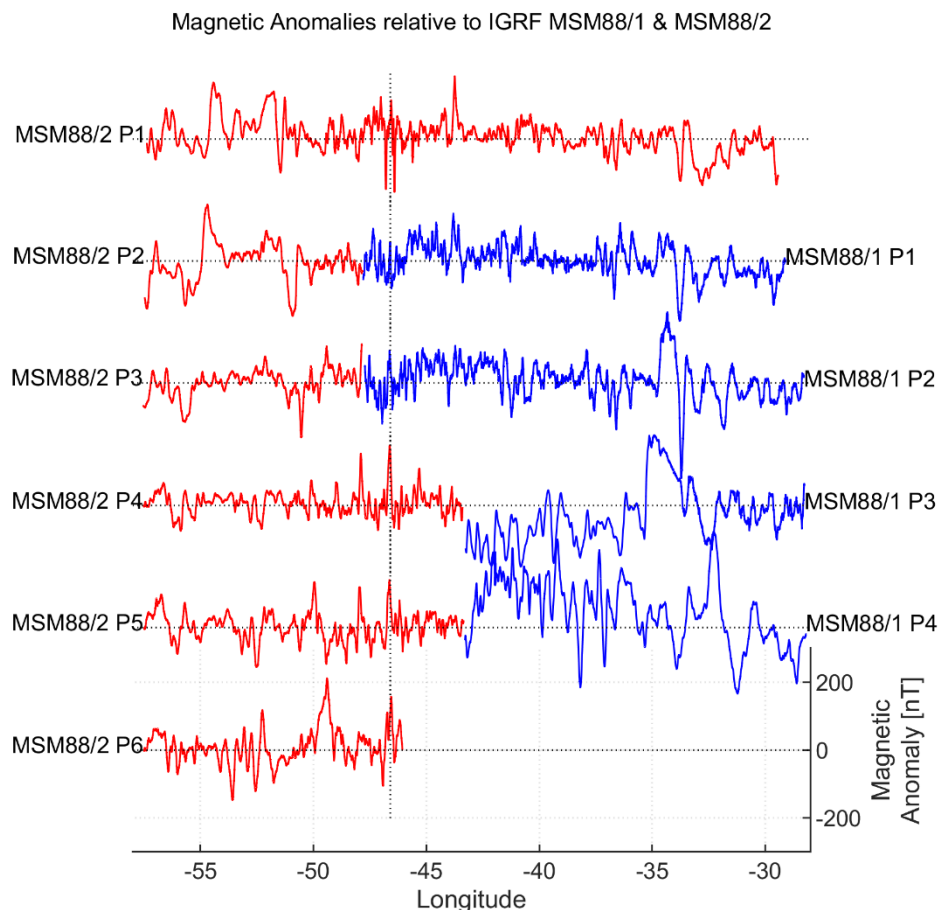


Figure 5.2: Stacked anomalies from MSM88/1 (blue) and MSM88/2 (red). The black solid vertical line marks the location of the MAR.

6 Station List MSM88

6.1 Overall Station List

Activity	Date/Time	Device	Action	Position	Position	Depth	Speed	Courses	Wind	Wind	Rope	Wind	Rope	Length	Comment
No.	[UTC]					[m]	[kn]	[°]	Direction	Velocity	m/s	kn	m	m	
0548892_1-SWP	2012.19.08:54	Sound Velocity Profiler	In the water	Lat	Lon										
				max depth/on ground		14° 36' 23.9" N	028° 13.93" W	5244.3	0	161.1	47.4	10.7	EL1	0	
0548892_1-SWP	2012.19.10:10	Sound Velocity Profiler	on deck	profile start		14° 36' 23.9" N	028° 13.93" W	5244.7	0	274.9	40.8	11.3	EL1	-14	
0548892_1-SWP	2012.19.10:34	Sound Velocity Profiler	profile start			14° 36' 42.2" N	028° 14.69" W	5225.1	0	265.9	48.4	10.9	ERROR	0	vs 10 kn; rwd = 275°
0548892_2-1-MW22	2012.19.16:30	Deep-sea Multibeam Echosounder	information			14° 41.22" N	029° 15.07" W	5409.7	0	278.7	50.9	10.7	ERROR	0	Unterbrechung Profil; Aussetzen Magnetometer
0548892_2-1-MW22	2012.19.18:28	Deep-sea Multibeam Echosounder	information			14° 43.09" N	029° 14.94" W	5407.1	0	271.5	49.7	10.4	ERROR	0	Fortsitzend Profil
0548892_2-1-MW22	2012.19.19:17	Deep-sea Multibeam Echosounder	information			14° 46.92" N	028° 18.45" W	3105.6	0	282.9	10.2	5.3	ERROR	0	Unterbrechung Profil
0548892_2-1-MW22	2012.19.19:25	Deep-sea Multibeam Echosounder	information			14° 48.48" N	028° 18.45" W	3055.4	0	280.1	10.5	6	ERROR	0	Fortsitzend Profil
0548892_2-1-MW22	2012.19.21:22	Deep-sea Multibeam Echosounder	profile end			14° 50.92" N	027° 19.79" W	5844.7	0	273.2	12.9	5.6	ERROR	0	
0548892_2-1-MW22	2012.19.21:27	Deep-sea Multibeam Echosounder	profile start			14° 52.32" N	028° 20.77" W	5221.2	0	272.1	12.2	5.3	ERROR	0	vs 10 kn; rwd = 275°
0548892_2-1-MW22	2012.19.26:30	Deep-sea Multibeam Echosounder	profile start			14° 41.22" N	029° 15.24" W	5411.1	0	277.4	3.7	11.3	ERROR	0	Unterbrechung Profil; Aussetzen Magnetometer
0548892_2-2-PTW	2012.19.28:28	Parasound	information			14° 41.22" N	029° 14.94" W	5225.1	0	271.5	49.7	10.4	ERROR	0	Fortsitzend Profil
0548892_2-2-PTW	2012.19.28:56	Parasound	profile end			14° 45.92" N	027° 18.46" W	5831.7	0	273.7	18.6	5.3	ERROR	0	Ausgetaktete Länge: 350 m
0548892_2-3-MAG	2012.19.29:28	Magnetometer	in the water			14° 41.82" N	029° 15.27" W	5411.7	0	273.7	39.3	10	ERROR	0	vs 10 kn; rwd = 275°
0548892_2-3-MAG	2012.19.29:32	Magnetometer	profile start			14° 43.09" N	029° 15.27" W	5407.1	0	271.5	49.7	10.4	ERROR	0	vs 10 kn; rwd = 275°
0548892_2-3-MAG	2012.19.29:40	Magnetometer	profile end			14° 50.01" N	027° 19.65" W	5845.3	0	275.1	15.3	6	ERROR	0	
0548892_2-3-MAG	2012.19.29:56	Magnetometer	profile start			14° 50.19" N	027° 19.65" W	5845.3	0	273.9	14.4	3.8	ERROR	0	
0548892_3-1-SWP	2012.19.30:02	Sound Velocity Profiler	in the water			16° 50.48" N	027° 10.86" W	5839.5	0	300.2	160.1	3.3	AMW	0	
0548892_3-1-SWP	2012.19.30:02	Sound Velocity Profiler	max depth/on ground			16° 50.48" N	027° 10.86" W	5844.6	0	298.2	146.9	3.8	AMW	-20	
0548892_3-1-SWP	2012.19.30:02	Sound Velocity Profiler	on deck			16° 50.48" N	027° 10.86" W	5843.2	0	100.7	182.2	3.1	ERROR	0	vs 10 kn; rwd = 275°
0548892_3-1-SWP	2012.19.30:02	Sound Velocity Profiler	profile start			16° 50.48" N	027° 10.86" W	5843.2	0	92.2	100.3	7.1	ERROR	0	vs 10 kn; rwd = 275°
0548892_3-1-SWP	2012.19.30:02	Sound Velocity Profiler	profile end			16° 51.65" N	027° 10.84" W	4093.4	0	101.7	180.2	3.1	ERROR	0	vs 10 kn; rwd = 275°
0548892_3-1-SWP	2012.19.30:51	Parasound	profile start			16° 51.65" N	027° 19.65" W	5411.7	0	275.1	15.3	6	ERROR	0	
0548892_3-1-SWP	2012.19.30:51	Parasound	profile end			16° 51.65" N	027° 19.65" W	5838.3	0	275.1	14.4	3.8	ERROR	0	
0548892_3-1-SWP	2012.19.30:56	Parasound	profile start			16° 52.95" N	027° 19.65" W	5845.3	0	273.9	14.4	3.8	ERROR	0	
0548892_3-1-SWP	2012.19.30:56	Parasound	profile end			16° 52.95" N	027° 19.65" W	5845.3	0	273.9	14.4	3.8	ERROR	0	
0548892_4-1-MW22	2012.19.31:36	Deep-sea Multibeam Echosounder	information			16° 52.95" N	027° 19.65" W	5845.3	0	101.8	180.8	3.1	ERROR	0	
0548892_4-1-MW22	2012.19.31:52	Deep-sea Multibeam Echosounder	profile start			16° 52.95" N	027° 19.65" W	5845.3	0	101.8	180.8	3.1	ERROR	0	
0548892_4-1-MW22	2012.19.31:52	Deep-sea Multibeam Echosounder	profile end			16° 53.22" N	027° 19.65" W	5845.3	0	101.8	180.4	4.6	ERROR	0	
0548892_4-1-MW22	2012.19.31:52	Deep-sea Multibeam Echosounder	profile start			16° 53.22" N	027° 19.65" W	5845.3	0	101.8	180.4	4.6	ERROR	0	
0548892_4-1-MW22	2012.19.31:52	Deep-sea Multibeam Echosounder	profile end			16° 53.22" N	027° 19.65" W	5845.3	0	101.8	180.4	4.6	ERROR	0	
0548892_4-1-MW22	2012.19.31:52	Deep-sea Multibeam Echosounder	profile start			16° 53.22" N	027° 19.65" W	5845.3	0	101.8	180.4	4.6	ERROR	0	
0548892_4-1-MW22	2012.19.31:52	Deep-sea Multibeam Echosounder	profile end			16° 53.22" N	027° 19.65" W	5845.3	0	101.8	180.4	4.6	ERROR	0	
0548892_4-1-MW22	2012.19.31:52	Deep-sea Multibeam Echosounder	profile start			16° 53.22" N	027° 19.65" W	5845.3	0	101.8	180.4	4.6	ERROR	0	
0548892_4-1-MW22	2012.19.31:52	Deep-sea Multibeam Echosounder	profile end			16° 53.22" N	027° 19.65" W	5845.3	0	101.8	180.4	4.6	ERROR	0	
0548892_4-1-MW22	2012.19.31:52	Deep-sea Multibeam Echosounder	profile start			16° 53.22" N	027° 19.65" W	5845.3	0	101.8	180.4	4.6	ERROR	0	
0548892_4-1-MW22	2012.19.31:52	Deep-sea Multibeam Echosounder	profile end			16° 53.22" N	027° 19.65" W	5845.3	0	101.8	180.4	4.6	ERROR	0	
0548892_4-1-MW22	2012.19.31:52	Deep-sea Multibeam Echosounder	profile start			16° 53.22" N	027° 19.65" W	5845.3	0	101.8	180.4	4.6	ERROR	0	
0548892_4-1-MW22	2012.19.31:52	Deep-sea Multibeam Echosounder	profile end			16° 53.22" N	027° 19.65" W	5845.3	0	101.8	180.4	4.6	ERROR	0	
0548892_4-1-MW22	2012.19.31:52	Deep-sea Multibeam Echosounder	profile start			16° 53.22" N	027° 19.65" W	5845.3	0	101.8	180.4	4.6	ERROR	0	
0548892_4-1-MW22	2012.19.31:52	Deep-sea Multibeam Echosounder	profile end			16° 53.22" N	027° 19.65" W	5845.3	0	101.8	180.4	4.6	ERROR	0	
0548892_4-1-MW22	2012.19.31:52	Deep-sea Multibeam Echosounder	profile start			16° 53.22" N	027° 19.65" W	5845.3	0	101.8	180.4	4.6	ERROR	0	
0548892_4-1-MW22	2012.19.31:52	Deep-sea Multibeam Echosounder	profile end			16° 53.22" N	027° 19.65" W	5845.3	0	101.8	180.4	4.6	ERROR	0	
0548892_4-1-MW22	2012.19.31:52	Deep-sea Multibeam Echosounder	profile start			16° 53.22" N	027° 19.65" W	5845.3	0	101.8	180.4	4.6	ERROR	0	
0548892_4-1-MW22	2012.19.31:52	Deep-sea Multibeam Echosounder	profile end			16° 53.22" N	027° 19.65" W	5845.3	0	101.8	180.4	4.6	ERROR	0	
0548892_4-1-MW22	2012.19.31:52	Deep-sea Multibeam Echosounder	profile start			16° 53.22" N	027° 19.65" W	5845.3	0	101.8	180.4	4.6	ERROR	0	
0548892_4-1-MW22	2012.19.31:52	Deep-sea Multibeam Echosounder	profile end			16° 53.22" N	027° 19.65" W	5845.3	0	101.8	180.4	4.6	ERROR	0	
0548892_4-1-MW22	2012.19.31:52	Deep-sea Multibeam Echosounder	profile start			16° 53.22" N	027° 19.65" W	5845.3	0	101.8	180.4	4.6	ERROR	0	
0548892_4-1-MW22	2012.19.31:52	Deep-sea Multibeam Echosounder	profile end			16° 53.22" N	027° 19.65" W	5845.3	0	101.8	180.4	4.6	ERROR	0	
0548892_4-1-MW22	2012.19.31:52	Deep-sea Multibeam Echosounder	profile start			16° 53.22" N	027° 19.65" W	5845.3	0	101.8	180.4	4.6	ERROR	0	
0548892_4-1-MW22	2012.19.31:52	Deep-sea Multibeam Echosounder	profile end			16° 53.22" N	027° 19.65" W	5845.3	0	101.8	180.4	4.6	ERROR	0	
0548892_4-1-MW22	2012.19.31:52	Deep-sea Multibeam Echosounder	profile start			16° 53.22" N	027° 19.65" W	5845.3	0	101.8	180.4	4.6	ERROR	0	
0548892_4-1-MW22	2012.19.31:52	Deep-sea Multibeam Echosounder	profile end			16° 53.22" N	027° 19.65" W	5845.3	0	101.8	180.4	4.6	ERROR	0	
0548892_4-1-MW22	2012.19.31:52	Deep-sea Multibeam Echosounder	profile start			16° 53.22" N	027° 19.65" W	5845.3	0	101.8	180.4	4.6	ERROR	0	
0548892_4-1-MW22	2012.19.31:52	Deep-sea Multibeam Echosounder	profile end			16° 53.22" N	027° 19.65" W	5845.3	0	101.8	180.4	4.6	ERROR	0	
0548892_4-1-MW22	2012.19.31:52	Deep-sea Multibeam Echosounder	profile start			16° 53.22" N	027° 19.65" W	5845.3	0	101.8	180.4	4.6	ERROR	0	
0548892_4-1-MW22	2012.19.31:52	Deep-sea Multibeam Echosounder	profile end			16° 53.22" N	027° 19.65" W	5845.3	0	101.8	180.4	4.6	ERROR	0	
0548892_4-1-MW22	2012.19.31:52	Deep-sea Multibeam Echosounder	profile start			16° 53.22" N	027° 19.65" W	5845.3	0	101.8	180.4	4.6	ERROR	0	
0548892_4-1-MW22	2012.19.31:52	Deep-sea Multibeam Echosounder	profile end			16° 53.22" N	027° 19.65" W	5845.3	0	101.8	180.4	4.6	ERROR	0	
0548892_4-1-MW22	2012.19.31:52	Deep-sea Multibeam Echosounder	profile start			16° 53.22" N	027° 19.65" W	5845.3	0	101.8	180.4	4.6	ERROR	0	
0548892_4-1-MW22	2012.19.31:52	Deep-sea Multibeam Echosounder	profile end			16° 53.22" N	027° 19.65" W	5845.3	0	101.8	180.4	4.6	ERROR	0	
0548892_4-1-MW22	2012.19.31:52	Deep-sea Multibeam Echosounder	profile start			16° 53.22" N	027° 19.65" W	5845.3	0	101.8	180.4	4.6	ERROR	0	
0548892_4-1-MW22	2012.19.31:52	Deep-sea Multibeam Echosounder	profile end			16° 53.22" N	027° 19.65" W	5845.3	0	101.8	180.4	4.6	ERROR	0	
0548892_4-1-MW22	2012.19.31:52	Deep-sea Multibeam Echosounder	profile start			16° 53.22" N	027° 19.65" W	5845.3	0	101.8					

MSM88/8-8.1/M422	10.01.2017:10	Dreieck-Mulheim-Echosounder	alt course	15°51'48"N 05°14'09"W 4672.1	10	89.4	45.7	12.8	ERROR	0	rwk-095*
MSM88/8-8.1/M422	11.01.2019:10	Dreieck-Mulheim-Echosounder	profile end	15°53'24"N 04°52'57"W 3488.1	10	93.6	65.6	12.8	ERROR	0	rwk-095*
MSM88/8-8.2/P70	09.01.2011:54	Profilmeter	profile start	16°13'59"N 05°20'52"W 5016.8	10	98.1	72.7	12.9	ERROR	0	ve 10 m; rwk-095*
MSM88/8-8.2/P70	09.01.2012:38	Profilmeter	alt course	15°50'28"N 05°14'09"W 4672.1	10	91.1	53.2	14.7	ERROR	0	rwk-095*
MSM88/8-8.2/P70	10.01.2017:10	Parasound	alt course	15°51'48"N 04°57'41"W 3488.1	10	93.6	65.6	12.8	ERROR	0	rwk-095*
MSM88/8-8.2/P70	11.01.2019:10	Parasound	profile end	15°53'24"N 04°52'57"W 3488.1	10	93.6	65.6	12.8	ERROR	0	rwk-095*
MSM88/8-8.3/MAG	08.01.2011:22	Magnetometer	profile start	16°20'29"N 05°77'31.99"W 0	10	180.7	79.8	14.3	ERROR	0	ve 10 m; rwk-095*
MSM88/8-8.3/MAG	08.01.2011:22	Magnetometer	information	16°20'66.1"N 05°77'31.99"W 0	10	178.3	70.7	13.5	ERROR	0	Gef. von MSM88/2-3 nach im Wasser
MSM88/8-8.3/MAG	09.01.2012:38	Magnetometer	alt course	15°50'82.5"N 05°1°40'46"W 5124.3	10	91	53.2	14.7	ERROR	0	rwk-095*
MSM88/8-8.3/MAG	10.01.2017:10	Magnetometer	information	15°51'49.5"N 04°57'14.09"W 4672.1	10	89.4	45.7	12.8	ERROR	0	rwk-095*
MSM88/8-8.3/MAG	11.01.2017:40	Magnetometer	profile end	15°34'7.65"N 04°53'25.5"W 3488.1	5	89.6	61.4	16.1	ERROR	0	Beim Einholen
MSM88/8-8.3/MAG	11.01.2017:50	Magnetometer	information	15°34'67.5"N 04°56'02.501"W 3758.3	5	96.6	77.8	7.4	ERROR	0	
MSM88/8-8.3/MAG	11.01.2018:11	Magnetometer	on deck	15°34'52.0"N 04°56'31.05"W 3758.3	5	85.8	64.8	12.4	ERROR	0	
MSM88/8-9.1/M422	11.01.2019:45	Dreieck-Mulheim-Echosounder	profile start	15°28'64.5"N 04°57'13.19"W 3489.3	13	227.7	70.2	11.9	ERROR	0	ve 12.5 m; rwk-275*
MSM88/8-9.1/M422	12.01.2019:52	Dreieck-Mulheim-Echosounder	alt course	15°46'58.9"N 05°07'10.98"W 4672.2	12	269.5	65.5	15.3	ERROR	0	
MSM88/8-9.1/M422	12.01.2019:55	Dreieck-Mulheim-Echosounder	alt course	15°46'65.1"N 05°21'18.53"W 3489.4	13	227.8	70.4	13.8	ERROR	0	rwk-275*
MSM88/8-9.1/M422	12.01.2019:59	Dreieck-Mulheim-Echosounder	information	15°56'48.0"N 05°41'34.90"W 4662.3	13	278.5	65.9	12	ERROR	0	Unterbrech. Profil technische Probleme EM422
MSM88/8-9.1/M422	13.01.2019:56	Dreieck-Mulheim-Echosounder	information	15°54'54.0"N 05°41'11.38"W 4649.0	12	269.5	53.8	16	ERROR	0	Fortsetzung Profil
MSM88/8-9.1/M422	13.01.2019:56	Dreieck-Mulheim-Echosounder	profile end	16°09'48.8"N 05°57'30.95"W 5261.4	12	275.1	58.9	15	ERROR	0	ve 12.5 m; rwk-275*
MSM88/8-9.2/P70	11.01.2017:50	Parasound	profile start	15°40'55.7"N 04°48'55.23"W 4483.4	13	257.5	64.5	14.2	ERROR	0	
MSM88/8-9.2/P70	12.01.2017:12	Parasound	alt course	15°46'58.9"N 05°07'10.98"W 4672.2	12	269.5	64.5	13.3	ERROR	0	rwk-275*
MSM88/8-9.2/P70	12.01.2017:45	Parasound	alt course	15°46'65.1"N 05°27'18.53"W 3489.4	13	273.8	70.4	13.8	ERROR	0	
MSM88/8-9.2/P70	12.01.2017:46	Parasound	information	15°54'58.2"N 05°47'13.01"W 5066.2	13	278.5	65.3	12	ERROR	0	Unterbrech. Profil technische Probleme EM422
MSM88/8-9.2/P70	13.01.2017:36	Parasound	information	15°54'50.7"N 05°47'11.38"W 5149.0	12	268.5	51.8	16	ERROR	0	Fortsetzung Profil
MSM88/8-9.2/P70	13.01.2017:46	Parasound	profile end	16°09'48.8"N 05°57'30.95"W 5261.2	12	275.1	58.9	15	ERROR	0	Forsetzung Profil

7 Data and Sample Storage and Availability

The hydroacoustic data (multibeam, parasound) of the work area will be placed in the GEOMAR data management system to ensure safe archiving. The multibeam data will also directly be published in PANGAEA with unrestricted access and also in the IHO DCDB. The magnetometer data has been recorded by Hamburg University and will be stored in the respective archive. Data can be immediately shared for cooperation.

The scientific work performed during the cruise strictly adhered to the “Maßnahmen im Hinblick auf die Erklärung zu einer verantwortungsvollen Meeresforschung” as well as the OSPAR code of conduct for responsible marine research in the deep seas and high seas of the OSPAR Maritime Area. Acoustic measurements were performed in a way to minimize the impact on marine mammals by activating the mammal protection system of the Kongsberg multibeam system. There was no duplication of previous studies, since the majority of the working area was unmapped. The bathymetry data will be published according to the FAIR data principles.

Table 8.1: Overview of data availability

Data type	Data archive	Available	Open access	Contact
Multibeam data (raw)	BSH, PANGAEA	February 2020 March 2020	yes yes	
Parasound data (raw)	BSH	February 2020	yes	
Magnetic data (raw)	DKRZ data base at University of Hamburg	February 2020	yes	Christian.huebscher@uni-hamburg.de

8 Acknowledgements

We sincerely thank the Captains Björn Maas (leg 1) and Ralf Schmidt (leg 2) and the professional crew of the MARIA S. MERIAN for their enthusiastic support during MSM88. The ship time of R/V MARIA S. MERIAN was provided by the Deutsche Forschungsgemeinschaft DFG. The participation of GEOMAR scientists was financed by the Helmholtz-Gemeinschaft.

9 References

- Allerton, S., and M.A. Tivey, 2001. Magnetic polarity structure of lower oceanic crust, *Geophys. Res. Lett.*, 28, 423-426.
- Harrison, C. G. A., Marine magnetic anomalies - the origin of the stripes, *Ann. Rev. Earth Planet. Sci.*, 15, 505-543, 1987.
- Marks, K.M., Smith, W.H.F., Sandwell, D.T., 2013. Significant improvements in marine gravity from ongoing satellite missions. *Marine Geophysical Researches* 34, 137-146.
- Mayer, L., Jakobsson, M., Allen, G., Dorschel, B., Falconer, R., Ferrini, V.L., Lamarche, G., Snaith, H., Weatherall, P., 2018. The Nippon Foundation - GEBCO Seabed 2030 Project: The quest to see the World's oceans completely mapped by 2030. *Geosciences* 8.
- Picard, K., Brooke, B.P., Harris, P.T., Siwabessy, P.J.W., Coffin, M.F., Tran, M., Spinoccia, M., Weales, J., Macmillan-Lawler, M., Sullivan, J., 2018. Malaysia Airlines flight MH370 search data reveal geomorphology and seafloor processes in the remote southeast Indian Ocean. *Marine Geology* 395, 301-319.
- Sandwell, D.T., Smith, W.H.F., 1997. Marine gravity anomaly from Geosat and ERS-1 satellite altimetry. *J. Geophys. Res.* 102, 10039-10054.
- Talwani, M., C. C. Windisch and M. G. 1971. Langseth, Reykjanes Ridge crest: A detailed geophysical study, *J. Geophys. Res.*, 76, 473-517.
- Wölfel, A.-C., Jencks, J., Johnston, G., Varner, J., Devey, C., 2017. Identifying deep-sea target areas for a pilot Atlantic seabed mapping project using GIS techniques. *J. Ocean Technn.* 12, 28-42.
- Wölfel, A.-C., Snaith, H., Amirebrahimi, S., Devey, C.W., Dorschel, B., Ferrini, V., Huvenne, V.A.I., Jakobsson, M., Jencks, J., Johnston, G., Lamarche, G., Mayer, L., Millar, D., Pedersen, T.H., Picard, K., Reitz, A., Schmitt, T., Visbeck, M., Weatherall, P., Wigley, R., 2019. Seafloor Mapping - The Challenge of a Truly Global Ocean Bathymetry. *Frontiers in Marine Science* 6.

10 Abbreviations

EEZ = exclusive economic zone

MAR = mid-Atlantic ridge

DAM = German Marine Research Alliance

11 Appendix - Selected Pictures of Samples

